Thermochimica Acta, 196 (1992) 255–265
Elsevier Science Publishers B.V., Amsterdam

The significance of the onset and final temperatures in the kinetic analysis of TG curves

D. Dollimore, T.A. Evans, Y.F. Lee, G.P. Pee and F.W. Wilburn
The Department of Chemistry, The University of Toledo, Toledo, OH 43606 (USA)

(Received 7 July 1991)

Abstract

The importance of the onset temperature has perhaps been unduly stressed in the literature. In many TG plots, it is seen that the final temperature is more significantly determined than the onset temperature. By reconstructing TG graphs from the predetermined set of Arrhenius parameters and applying different kinetic mechanisms to the calculations, it is apparent that the "sharpness" of the onset and final temperature is due to kinetic factors–especially the kinetic mechanism. Certain kinetic mechanism expressions lead to an asymptotic departure from the base line in a TG plot while others produce a very "sharp" approach to the final plateau. An inspection of these features can thereby indicate the probable kinetic mechanism of a TG plot.

INTRODUCTION

In reporting thermogravimetry (TG) experiments the importance of the onset temperature has perhaps been unduly stressed in the literature. It is usual to state the extrapolated onset temperature by drawing tangents as indicated in Fig. 1. However in many cases the computer work station allows the operator to make a practical choice by visual inspection. A cursory inspection of Fig. 1 shows that the final temperature of decomposition is often more sharply delineated than the onset or initial temperature. Typical shapes for TG plots (paying exaggerated attention to these two characteristic temperatures) are shown in Fig. 2. It would seem that the following "typical shapes" can be noted: (a) T_i (initial or onset temperature) and T_f (final temperature) sharp; (b) T_i diffuse and T_f sharp; (c) T_i sharp and T_f diffuse; (d) T_i and T_f both diffuse.

A cursory inspection of single-stage decomposition steps in many systems would suggest that a large number of these curves are characterized by a diffuse initial temperature and a sharp final temperature. However all four of the possible shapes of TG plots can be found in the literature. The corresponding differential thermogravimetry (DTG) plots for these characteristic TG plots are given in Fig. 3. The schematic plots show the peak width at half height or half width. The asymmetry of the curves is expressed

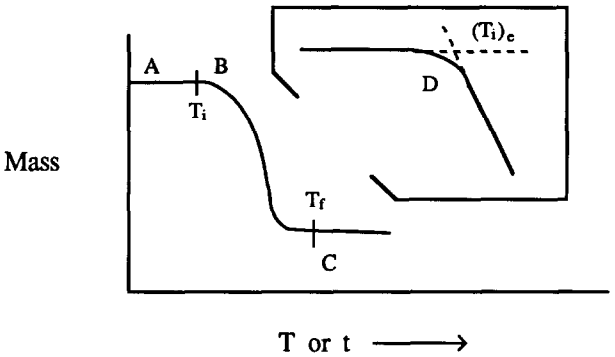

Fig. 1. Schematic TG curve: B, onset temperature, T_i; C, final temperature, T_f; D, extrapolated onset temperature, $(T_i)_e$.

as $\Delta \mathrm{Lo}T/\Delta \mathrm{Hi}T = T_p - \mathrm{Lo}T/\mathrm{Hi}T - T_p$ where T_p is the peak temperature, and LoT and HiT represent the low-temperature end and high-temperature end of the half width.

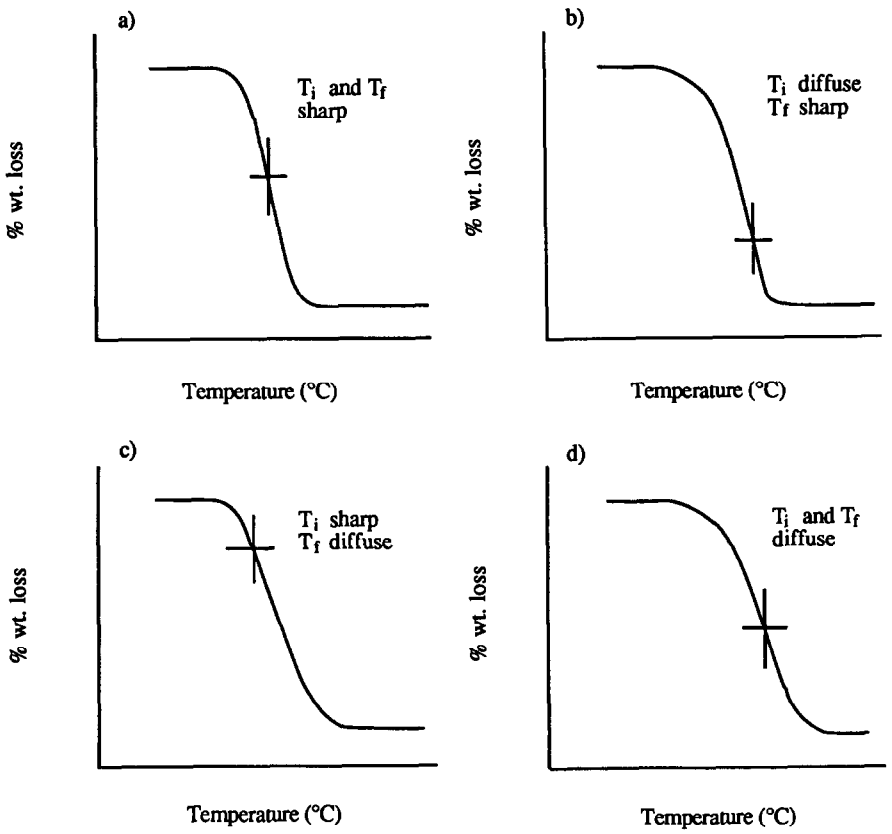

Fig. 2. Schematic representation of TG plots–typical shapes; +, point of maximum slope, i.e. $(\mathrm{d}\alpha/\mathrm{d}T)_{max}$.

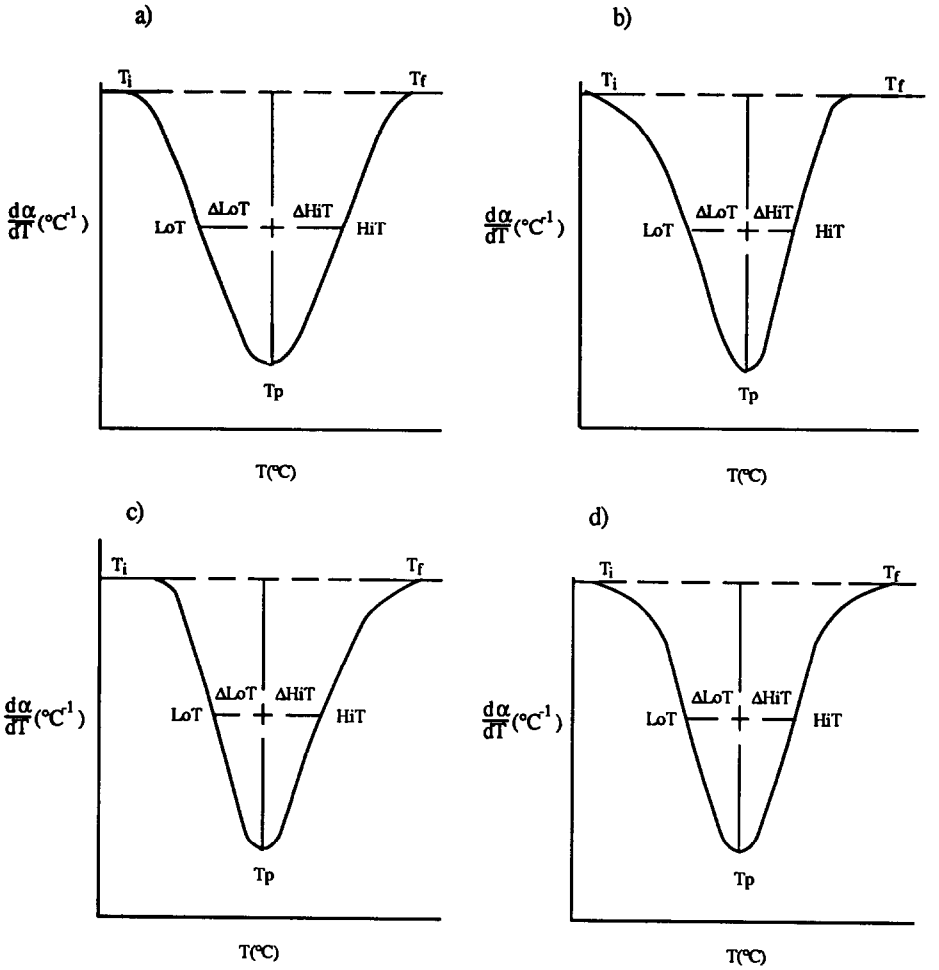

Fig. 3. Typical DTG plots corresponding to TG plots shown in Fig. 2.

In case (a), where both T_i and T_f are sharp, $\Delta LoT \approx \Delta HiT$. Similarly in case (d) where T_i and T_f are both diffuse, $\Delta LoT \approx \Delta HiT$. However for the case where T_f is sharp and T_i diffuse (Fig. 3b), $\Delta HiT < \Delta LoT$; and for the cases where T_i is sharp and T_f diffuse (Fig. 3c), $\Delta HiT > \Delta LoT$.

The imposition of a characteristic shape to the TG curve is kinetic in origin [1] and the above comments are qualitative in nature. The next step is to try and impose quantitative features on this picture.

KINETIC ANALYSIS OF TG CURVES

One can identify several different kinetic expressions to describe the behavior of solid state decompositions. Here the symbols used by the majority of investigators are used [2]. A computer program [3] using the differential form of these relationships based on the finite difference

TABLE 1

Reconstructed thermal analysis data for $E = 124$ kJ mol^{-1}, $A = 6.229 \times 10^{10}$ s^{-1} and heating rate = 15°C min^{-1} as a function of half width and shape factors for various mechanisms

Rkn Mech.	Half width (HiT − LoT) (°C)	T_p (°C)	LoT (°C)	HiT (°C)	ΔLoT (T_p − LoT) (°C)	ΔHiT (HiT − T_p) (°C)	$\frac{\Delta \text{Lo}T}{\Delta \text{Hi}T}$
A_2	20.0	273.4	226.0	246.0	11.40	8.600	1.326
A_3	14.0	237.3	230.0	244.0	7.300	6.700	1.089
A_4	10.0	236.8	232.0	242.0	4.800	5.200	0.9231
B_1	6.0	281.7	280.0	286.0	1.700	4.300	0.3953
R_2	28.0	226.0	208.0	236.0	18.00	10.000	1.800
R_3	32.0	219.6	200.0	232.0	19.60	12.40	1.581
D_1	24.0	237.7	214.0	238.0	23.70	0.3000	79.00
D_2	48.0	226.2	190.0	238.0	36.19	11.80	3.067
D_3	60.0	201.4	164.0	224.0	37.38	22.60	1.654
D_4	50.0	202.5	168.0	218.0	34.50	15.50	2.226
F_1	40.0	236.6	214.0	254.0	22.64	17.40	1.301
F_2	56.0	235.6	210.0	266.0	25.64	30.40	0.8434
F_3	70.0	246.2	220.0	290.0	26.22	43.80	0.5986

method, allowed α (fraction decomposed)–temperature plots to be developed given the Arrhenius parameters (A and E) and the kinetic mechanism. Here $A = 6.229 \times 10^{10}$ s^{-1} and $E = 124$ kJ mol^{-1}. At these values, the peak temperature, the half width and the asymmetry or shape factor terms are given in Table 1. For a perfect symmetry, $\Delta \text{Lo}T/\Delta \text{Hi}T = 1$. For the DTG plot in Fig. 3b, where $\Delta \text{Lo}T > \Delta \text{Hi}T$, $\Delta \text{Lo}T/\Delta \text{Hi}T$ is greater than unity; for the curve in Fig. 3c, where $\Delta \text{Lo}T < \Delta \text{Hi}T$, $\Delta \text{Lo}T/\Delta \text{Hi}T$ is less than unity. Inspection of Table 1 and of published plots of $d\alpha/dT$ against temperature [4,5] establishes the following facts regarding mechanism and T_i and T_f: mechanisms A_2, A_3 and A_4 have both T_i and T_f sharp; curves with T_i diffuse and T_f sharp include mechanisms R_2, R_3, D_1, D_2, D_3 and D_4; kinetic equations F_1, F_2 and F_3 belong to the group where both T_i and T_f are diffuse. Table 2 summarizes the various equations into three groups based on the onset and final temperatures.

TABLE 2

Characterization of various kinetic mechanisms based on the onset and final temperatures of DTG Curves

Group	Mechanisms	Characteristic features of T_i and T_f	$\frac{\Delta \text{Lo}T}{\Delta \text{Hi}T}$
A	A_2, A_3, A_4	T_i sharp, T_f sharp	≈ 1
B	R_2, R_3, D_1, D_2, D_3, D_4	T_i diffuse, T_f sharp	$\gg 1$
C	F_1, F_2, F_3	T_i diffuse, T_f diffuse	≈ 1

TABLE 3

Values of $(d\alpha/dT)_{max}$ and α_{max} for A_2 and D_2 mechanisms from a theoretical study of a variety of Arrhenius parameters and heating rates

β (°C min^{-1})	E (kJ mol^{-1})	A (s^{-1})	$(d\alpha/dT)_{max}$ (°C^{-1})	α_{max}
Mechanism A_2				
5	160	1×10^{15}	0.063	0.624
10	160	1×10^{15}	0.061	0.625
15	160	1×10^{15}	0.059	0.624
20	160	1×10^{15}	0.059	0.624
5	190	1×10^{15}	0.053	0.625
5	210	1×10^{15}	0.049	0.624
5	230	1×10^{15}	0.045	0.625
5	160	1×10^{17}	0.079	0.625
5	160	1×10^{19}	0.077	0.626
5	160	1×10^{21}	0.11	0.626
5	160	1×10^{23}	0.13	0.628
Mechanism D_2				
5	160	1×10^{15}	0.026	0.815
10	160	1×10^{15}	0.026	0.815
15	160	1×10^{15}	0.025	0.814
20	160	1×10^{15}	0.025	0.815
5	190	1×10^{15}	0.022	0.815
5	210	1×10^{15}	0.020	0.815
5	230	1×10^{15}	0.018	0.815
5	160	1×10^{17}	0.032	0.817
5	160	1×10^{19}	0.039	0.818
5	160	1×10^{21}	0.046	0.820
5	160	1×10^{23}	0.054	0.820

TABLE 4

Reasonable limits of $(d\alpha/dT)_{max}$, α_{max} and half width for various mechanisms obtained from theoretical study

Mechanism	$(d\alpha/dT)_{max}$ range (°C^{-1})	α_{max} range	Half width (°C)
P_1	0.09–0.16	1.00	< 12.00
E_1	0.62–1.85	0.98–1.00	–
A_2	0.04–0.13	0.62–0.63	14–32
A_3	0.01–0.19	0.63	12–22
A_4	0.08–0.24	0.63–0.65	< 10.00
B_1	0.11–0.24	0.54–0.55	8–12
R_2	0.03–0.09	0.73–0.74	24–34
R_3	0.03–0.08	0.69	20–42
D_1	0.03–0.09	1.00	24.00
D_2	0.02–0.05	0.81–0.82	24–78
D_3	0.01–0.04	0.67–0.68	30–70
D_4	0.02–0.05	0.75–0.76	38–80
F_1	0.02–0.07	0.62	20–60
F_2	0.01–0.04	0.48	22–94
F_3	0.01–0.03	0.40	> 66.00

To proceed further one needs to look at the half width and associated parameters connected with the asymmetry of the curve. In another paper [5], it is shown that α_{max}, the fraction decomposed at maximum rate decomposition and the half width can help in determining the mechanism. Table 3 provides evidence drawn from a theoretical study of a variety of Arrhenius parameters using the present computer program. Table 4 summarizes these data for all the mechanisms examined

It is observed that α_{max} does not change appreciably over a wide range of Arrhenius parameters and heating rates. However, the half width spans over a wider range. Therefore based on the shape of the DTG curve, coupled with α_{max} and half width, a methodology is developed to identify or narrow down the possible kinetic mechanisms.

METHODOLOGY

The program used in the kinetic analysis of the examples cited is written in FOXPRO based on the original computer program [3] written in BASIC. However, additional features such as the selection of the kinetic mechanism and the computation of the Arrhenius parameters are incorporated into the program.

A flow chart of the method for identifying the mechanism is given in Fig. 4. At the start, the data of % weight loss and temperature at 1°C intervals are obtained from the TG work station. A small temperature interval is desired because this gives better accuracy in determining the various parameters pertaining to the DTG curve. These data are input to the computer which converts the % weight loss to α values. The experimental

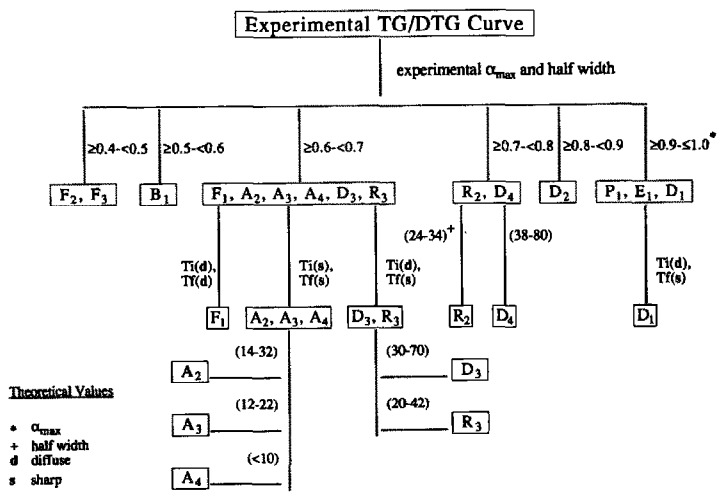

Fig. 4. Flow chart showing the procedures in recognizing the kinetic equations.

α_{max}, $(d\alpha/dT)_{max}$, HiT, LoT and half width are determined. The program then narrows down the possible equations by comparing the experimental α_{max} to the theoretical α_{max} range. It is observed that D_2 and B_1 can be identified based on the α_{max} alone. Both F_2 and F_3 cannot be further separated based on the half width and shape factor. However, the other mechanisms may be further separated. At this point, the computer will prompt the user for the shape factor, i.e. whether T_i and T_f are diffuse or sharp. This can easily be discerned from the DTG plot obtained from the TG work station.

In the $\geq 0.9 - \leq 1.0$ α_{max} range, D_1 can be discriminated by the shape factor alone. R_2 and D_4 can be separated by the half width, and in the α_{max} range of $\geq 0.6 - < 0.7$, the first-order equation can be distinguished from the Avrami–Erofeev equations and D_3/R_3 based on the shape factor. The other equations can be individually identified based on half width.

In the event when there is an overlapping of half width between two equations, the program will recommend both equations. If the experimental half width falls beyond the range stipulated, then recommendation is based on α_{max} and/or shape factor. The kinetic equation once identified will be used to calculate the specific rate constants. The activation energy and the pre-exponential factor can be calculated from an Arrhenius plot of ln k versus $1/T$. The Arrhenius parameters, together with the heating rate and kinetic equation are used to reconstruct the experimental TG and DTG curves. The theoretical parameters, i.e. the α_{max}, T_p, LoT, HiT and half width describing the asymmetry of the DTG curve are then compared to the values obtained experimentally. A close match indicates a correct choice of the kinetic equation.

Three examples of mechanism identification based on the above methodology are given. These include the dehydration of calcium oxalate monohydrate, decomposition of limestone and decomposition of zinc oxalate.

Dehydration of calcium oxalate monohydrate

$$CaC_2O_4 \cdot H_2O \rightarrow CaC_2O_4 + H_2O$$

The various experimental parameters pertaining to the DTG curve are given in Table 5a. From Fig. 5, it is observed that this plot belongs to group B (Table 2) which has T_i diffuse and T_f sharp. Also, ΔLoT/ΔHiT is larger than unity which is consistent with the theoretical study. Following the flow chart and based on the experimental α_{max} alone, R_2 and D_4 equations are favored. Because both R_2 and D_4 equations have the same characteristic shape factor, i.e. T_i diffuse and T_f sharp, further separation between these two equations is based on their half widths. The experimental half width is 52.3°C which indicates that D_4 mechanism is more favored.

TABLE 5

Parameters describing the asymmetry of the DTG curve for the dehydration of calcium oxalate monohydrate at 20°C min^{-1} in air

(a) Experimental								
α_{max}	$(d\alpha/dT)_{max}$ ($°C^{-1}$)	T_p (°C)	LoT (°C)	HiT (°C)	Half width (°C)	ΔLoT/ ΔHiT	T_i	T_f
0.787	0.0203	237.2	198.7	251.0	52.3	2.79	Diffuse	Sharp
(b) Theoretical								
Mechanism	α_{max}	T_p (°C)	LoT (°C)	HiT (°C)	Half width (°C)			
R_2	0.718	214.8	177	234	65			
D_4	0.748	237.7	205	255	50			

For comparison, both the Arrhenius parameters for R_2 and D_4 were used to reconstruct the experimental TG curve. Table 5b shows the theoretical parameters obtained. When one compares the theoretical and experimental parameters, D_4 mechanism gives a better reconstruction of the TG curve. Hence, the dehydration of calcium oxalate under the present experimental conditions followed a D_4 mechanism with an activation energy of 143.3 kJ mol^{-1} and a pre-exponential factor of 9.31×10^{11} s^{-1}.

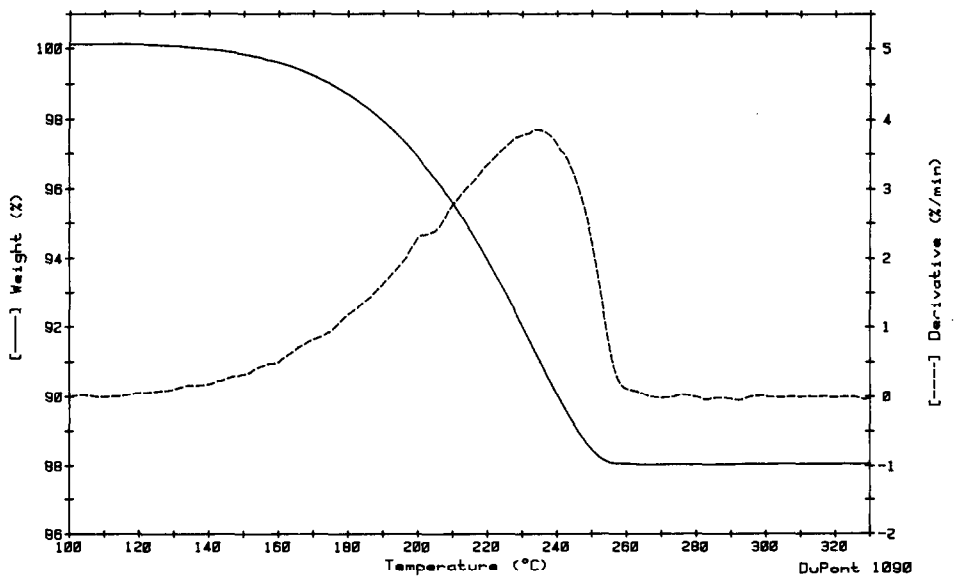

Fig. 5. TG and DTG curves for the dehydration of calcium oxalate monohydrate at 20°C min^{-1} in dynamic air.

TABLE 6

Parameters describing the asymmetry of the DTG curve for the decomposition of limestone at 10°C min^{-1} in air

(a) Experimental								
α_{max}	$(d\alpha/dT)_{max}$ ($°C^{-1}$)	T_p (°C)	LoT (°C)	HiT (°C)	Half width (°C)	ΔLoT/ΔHiT	T_i	T_f
0.678	0.0110	814.2	757.4	845.4	88.0	1.82	Diffuse	Sharp
(b) Theoretical								
Mechanism	α_{max}	T_p (°C)	LoT (°C)	HiT (°C)	Half width (°C)			
R_3	0.673	817.9	762.0	851.0	89.0			
D_3	0.682	818.7	670.0	819.0	149			

Decomposition of limestone

$$CaCO_3 \rightarrow CaO + CO_2$$

The experimental parameters are given in Table 6a. A glance at Fig. 6 shows that T_i is diffuse and T_f is sharp. Again, following the flow chart, the possible mechanisms from the experimental α_{max} are F_1, A_2, A_3, A_4, D_3 and R_3. Because the curve belongs to group B, the Avrami–Erofeev and

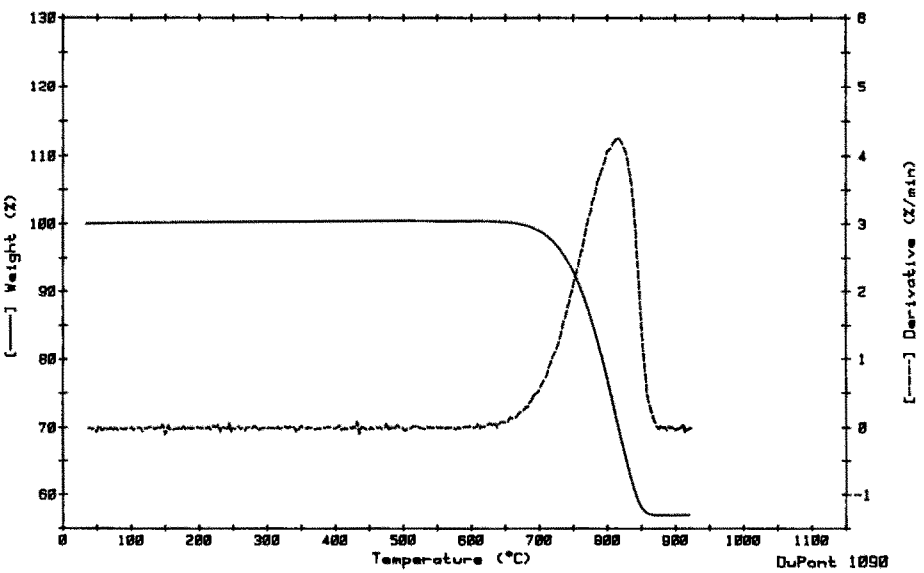

Fig. 6. TG and DTG plots for the decomposition of limestone at 10°C min^{-1} in dynamic air.

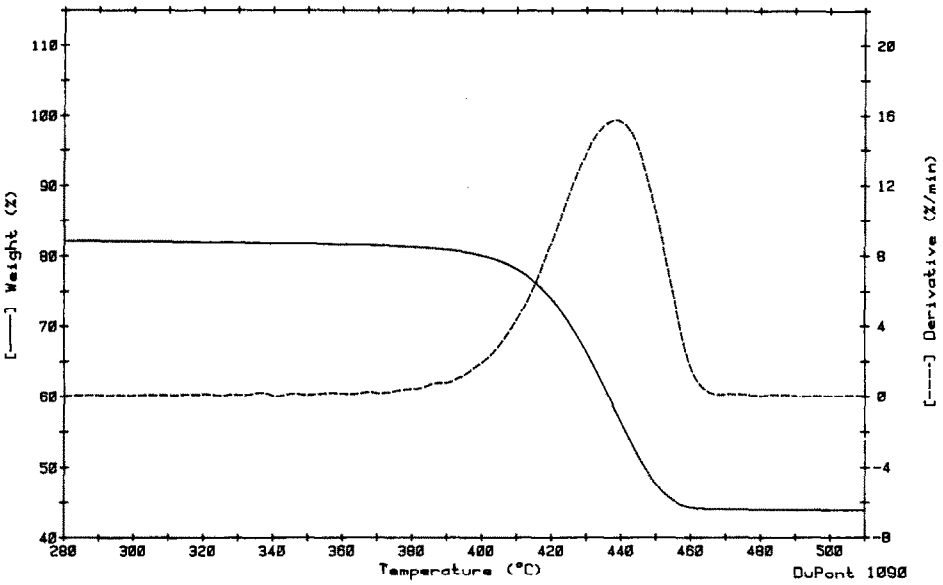

Fig. 7. TG and DTG traces for the decomposition of zinc oxalate at 15°C min^{-1} in dynamic air.

the first-order equations are disregarded. However, in this case, the experimental half width (88.0°C) is not within the theoretical range, thus further separation between these two equations is not feasible and the program recommends both D_3 and R_3 as the possible mechanism.

From Table 6b, the R_3 mechanism is a better choice to describe the decomposition. The Arrhenius parameters obtained are $E = 205.7$ kJ mol^{-1} and $A = 8.41 \times 10^6$ s^{-1}.

TABLE 7

Parameters of the DTG curve for the decomposition of zinc oxalate at 15°C min^{-1} in air

(a) Experimental								
α_{max}	$(d\alpha/dT)_{max}$ ($°C^{-1}$)	T_p (°C)	LoT (°C)	HiT (°C)	Half width (°C)	ΔLoT/ ΔHiT	T_i	T_f
0.625	0.0301	438.2	421.7	452.7	31.0	1.14	Diffuse	Diffuse
(b) Theoretical								
Mechanism	α_{max}	T_p (°C)	LoT (°C)	HiT (°C)	Half width (°C)			
F_1	0.615	440.0	417.0	457.0	40.0			

Decomposition of zinc oxalate

$ZnC_2O_4 \rightarrow ZnO + CO + CO_2$

In this example, the mechanism identification is rather straightforward. From Fig. 7, it is observed that both T_i and T_f are diffuse and $\Delta LoT/\Delta HiT$ is ≈ 1 (Table 7a). Because the experimental α_{max} falls between the range $\geq 0.6 - < 0.7$, the F_1 mechanism is the obvious choice. Table 7b shows the theoretical parameters of the DTG curve which are close in comparison to the experimental data. The activation energy is 252.9 kJ mol^{-1} and the pre-exponential factor is 5.03×10^{16} s^{-1}.

CONCLUSION

The method outlined in the kinetic analysis of TG and DTG curves is based on the asymmetry or the shape of the curves. The asymmetry is described both qualitatively and quantitatively. The qualitative approach separates the various kinetic equations into three groups by their characteristic onset and final temperatures. The quantitative approach utilizes parameters such as α_{max}, T_p, LoT, HiT and half width pertaining to the DTG curve.

The great advantage of this method of mechanism identification is shown by the three examples cited. A cursory inspection of the shapes of the curves will immediately narrow down the numbers of possible equations for consideration. In addition, the various parameters describing the DTG curve can be obtained easily without extensive computation.

REFERENCES

1 J. Šesták, V. Satava and W.W. Wendlandt, Thermochim. Acta, 7 (1973) 333.
2 M.E. Brown, D. Dollimore and A.K. Galwey, in C.H. Bamford and C.F.H. Tippers (Eds.), Reactions in the Solid State, Vol 22, Chemical Kinetics, Elsevier, Amsterdam, 1980, pp. 340.
3 D. Dollimore, T.A. Evans, Y.F. Lee and F.W. Wilburn, Thermochim. Acta, 188 (1991) 77.
4 M.E. Brown, Introduction to Thermal Analysis, Chapman and Hall, London, 1988, 147 pp.
5 D. Dollimore, T.A. Evans, Y.F. Lee and F.W. Wilburn, Proc. 19th North American Thermal Analysis Soc., 1990, p. 397.